Secondary Load Paths in Bridge Systems

ROLA L. IDRISS AND KENNETH R. WHITE

Abstract

Although most structural systems are designed as a series of individual elements, they will in fact respond to load as a rather complex integration of these elements. The load is transmitted through a combination of members which resist loads in proportion to their relative stiffness. These types of structures are said to have multiple load paths. Redundant load paths have not been normally considered in the design of structures. However, the consideration of secondary load paths can be a major factor in the assessment of the load carrying capacity of a damaged structure. This paper takes a further look at the reserve strength present in a multi-girder bridge system, and investigates the behavior of a damaged superstructure, the redistribution of loads, and the secondary load paths along which the load is transmitted when a damage occurs in the structure. Limit analysis was used to predict the overload behavior of a simply supported concrete slab-steel girder highway bridge system. The bridge superstructure was modeled as grid and grid framework elements. The experimental results from tests to failure on four large scale bridge models were used to verify the computer approach.

In order to study the response of a distressed bridge, a mathematical model consisting of four girders was analyzed. Three different finite element models were used to investigate the following conditions:

1. No damage in the superstructure.
2. Localized flange losses in a girder.
3. Crack in a girder.

Results are given in terms of load deflection curves for the three models.

Introduction

Evaluation of the load capacity of existing bridges is a major concern for highway agencies throughout the united states. A very important factor in the evaluation of a bridge is the determination of it's load carrying capacity. Bridge engineers are increasingly concerned about the overloading of highway bridges, due to the fact that many of these bridges are loaded beyond levels for which they were originally designed. Another difficult situation arises when a structure is rated deficient, and the decision has to be made concerning posting it, closing it, or replacing it.

Although most structural systems are designed as a series of elements, they generally behave as a system in which loads are transferred through a combination of members that resist loads in proportion to their relative stiffness. These types of structures are said to have multiple load paths. The proportion of load carried by each path is a function of the load location and intensity, as well as the relative stiffness of the various paths. Redundant load paths have not been normally considered in the design of structures. However the consideration of secondary load paths can be a major factor in the assessment of a damaged superstructure.

Typical steel stringer bridges are rather highly redundant structures. The reason for this is that although the girders are designed as line elements, they are continuously connected to a common concrete deck and to each other at close intervals with rather strong diaphragms, as well as bottom flange bracing in many instances. None of these elements are specifically recognized in the typical design calculations for live load.

Information on the behavior of a damaged structure is scarce; the influence of redundancy on the load capacity of such a structure has not been quantified yet. In this paper we further investigate the reserve strength present in a multi-girder bridge system, and the effects of deterioration on such a structure. To study the effects of deterioration, different types of damages are modeled into the structure, the reserve strength assessed, and the load redistribution and structural response of the bridge monitored.

Analytical Approach

To perform the analysis, limit analysis by the displacement method was used. Limit analysis by the displacement method was first introduced by Wang (1); this technique is simple, yet effective for the study of large systems in bending; it combines matrix displacement method and plastic analysis; plastic hinges are accounted for by modification of the members stiffness matrices.

The general procedure is as follows:

- An elastic analysis of the structure subjected to a given set of proportionate loads is made. The allowable load factor at each member end is computed as the ratio of the plastic moment capacity at the point to the end moment caused by the proportionate loads. The smallest of all the allowable load factors thus computed is the first stage load factor for the entire structure, and the location of the first plastic hinge.
- A second analysis of the modified structure, in which there is now one plastic hinge, is made for the proportionate loads. The point by which the second stage load factor is controlled is the location of the second plastic hinge. These processes are repeated until an unstable structure is encountered. The ultimate load factor is the sum of the load factors in all stages. The end moments are determined in the same manner.

Analytical Model

The beam and slab bridge superstructure is modeled by a system of grid and grid framework elements, as shown in figure 2. Grid framework elements were first investigated by Yettram and Hussain (2), and later applied by Traina (3) to the study of large flat plate structural systems in bending. The deflections and moments obtained by use of these models were found to converge to the exact mathematical solution as the mesh was refined. The concrete slab is modeled by equivalent grid plate elements, while the steel girders and diaphragms are modeled by grid elements. These compatible finite elements are connected thru their common nodes. This technique and analytical model were used successfully in previous studies by McCarthy (4) and Melhem (5) to predict the elastic-plastic response of concrete slab steel girder bridges. The results of the analytical study were checked against a number of failure experiments on bridge models . The analytical results compared well with the experimental data.

The limit analysis by the displacement method was further refined to accommodate full scale bridge modeling, including dead load, live load as well as impact. Dead load is applied gradually, and live load is applied as a set of concentrated proportional loads simulating a truck loading with the truck wheel configuration but only a fraction of the actual weight; this set of concentrated live loads is then incremented in the limit analysis, and live load factors are given at every cycle along with all the system flexural response: deflections, rotations, and plastic hinge formation.

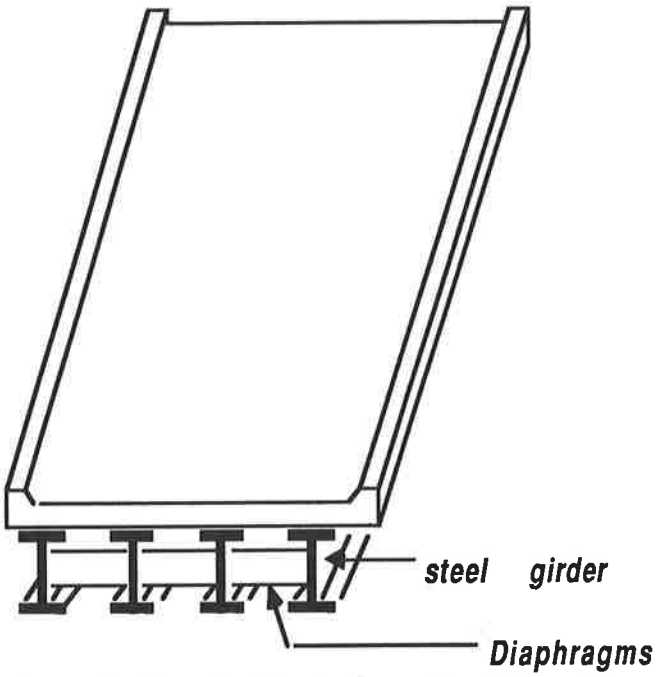

Figure 1. Typical I-Beam Superstructure

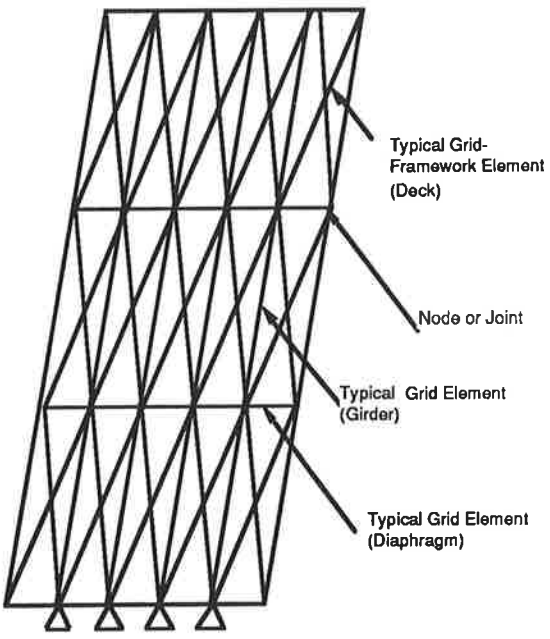

Figure 2. Typical Finite Element Arrangement .

Analytical vs Experimental Results

Analytical results were compared to experimental results from tests to failure on four bridges from the AASHTO road test (15) conducted in the early 60s. Four bridges were studied: 1A, 9A, 9B, and 3B. The first three were non composite bridges, while the last one was composite.

The four bridges had similar geometry; but differed in the beam sizes, the length and presence or absence of cover plates; each bridge superstructure consisted of three identical beams; the nominal sizes of the rolled sections and the length of the cover plates are given in table 1. The beams were simply supported, had a 50 ft span and carried a reinforced concrete slab 6.5 in thick and 15 ft wide.

Table 1. AASHTO Bridges beam sizes.

Bridge		Beam size	Length of cover plates (centered about midspan)	
Designation	Type		Top	Bottom
1A	Non Composite	18WF55		20 ft 6 in
9A,9B	Non Composite	18WF96	17 ft 0 in	17 ft 0 in
3B	Composite	18WF60		18 ft 6 in

Tests to failure were carried out with increments of loads applied with several overload vehicles. Permanent deformations accumulated rapidly with each increment of load after the load causing the first large permanent set.

In the computer simulation, each bridge was loaded with a proportionate set of concentrated live loads. These loads simulate the overload vehicle that caused first large permanent set in the bridge, with the same wheel configuration, but only a fraction of the actual weight. The truck was positioned to cause maximum bending moment at midspan. Analytical and experimental curves as shown in figures 3, 4, 5 and 6 compared very favorably up to the load that caused the first large permanent set (load factor of 1).

The analytical simulation was successful in predicting the plastic flow in the bridges; for bridges 1A, 9A, and 9B heavy yielding in the girders at sections near the ends of the cover plates, with full plastic hinges forming in these locations at failure. Composite bridge 3B showed excessive cracking in the slab and yielding of the girders at the ends of the cover plates that later formed plastic hinges. The analytical simulation for bridge 3B shows the slab reaching its plastic moment capacity first near the ends of the cover plates, then towards midspan of the bridge, which would be in agreement with the extensive cracks observed in the slab, and the formation of plastic hinges at the ends of the cover plates.

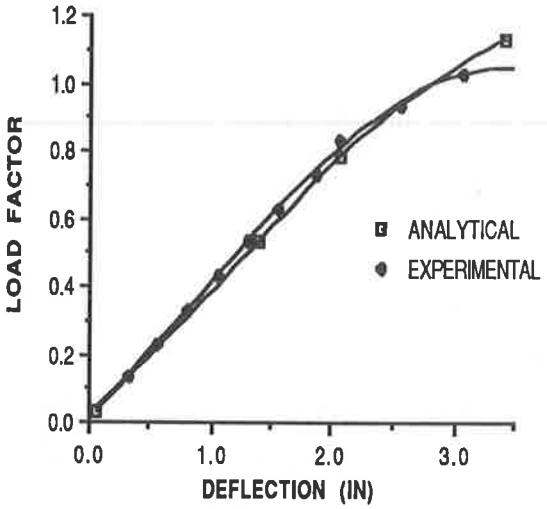

Figure 3. AASHTO Bridge 1A. Analytical vs experimental load-deflection curves.

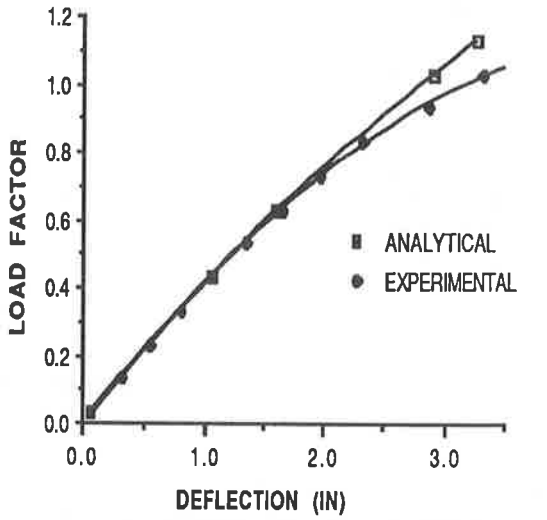

Figure 4. AASHTO Bridge 9A. Analytical vs experimental load-deflection curves.

The analytical simulation and actual experimental results showed good agreement in predicting load-deflection response up to the load that caused the first large permanent set; the analytical simulation was able to predict quite accurately the plastic flow in the structure. Experimental and analytical results disagreed when we compared the rate at which the deflection increased after the first large permanent set.

After the load that caused the first large permanent set (or decrease in stiffness), the actual structure showed a much greater deflection than the analytical model did.

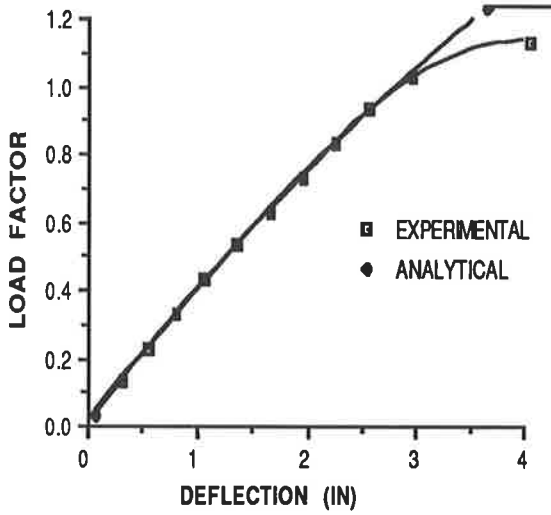

Figure 5. AASHTO Bridge 9B. Analytical vs experimental load-deflection curves.

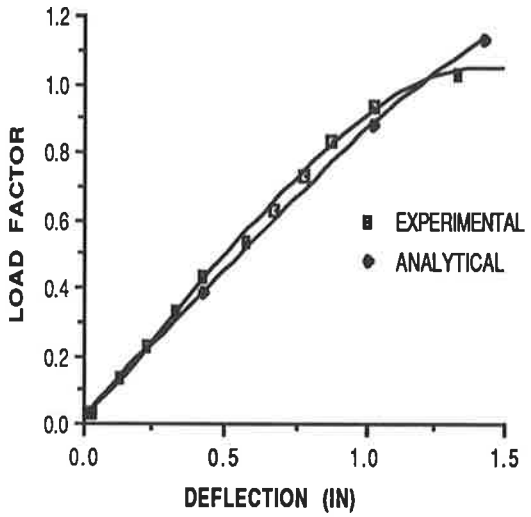

Figure 6. AASHTO Bridge 3B. Analytical vs experimental load-deflection curves.

Effects of deterioration:

In order to assess the effects of deterioration on the behavior of a concrete slab, multi-girder bridge superstructure, two multi-girder systems were examined. They consist of four main longitudinal girders, with diaphragms at ends and midspan. The roadway is a 28 ft wide, 8 in thick reinforced concrete deck; figure 7 shows a typical bridge cross section; girder sizes for span length of 50 ft and 180 ft are shown in table 2.

Table 2. Beam sizes, 50 ft and 180 ft simple span bridges.

Bridge		Beam Size
Span	Type	
50 ft	Non Composite	W36X182
180 ft	composite	Top Flange: 5/8 X 14 Web: 1/2 X 125 Bottom Flange: 1 1/4 X18 (for the72' midspan section) and 15/16 X 18 (for the two 54' endspan sections)

The 50 ft span bridge is non composite, while the 180 ft bridge is composite .

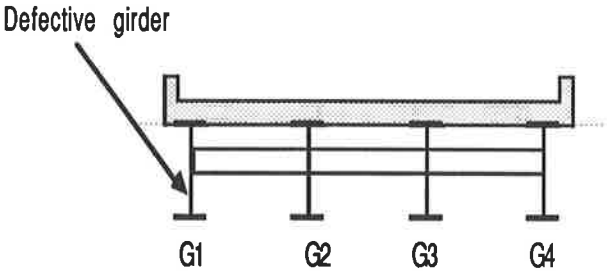

Figure 7. Typical Cross Section.

Three types of defects were modeled:

- Flange losses: 50% and 100% lower flange section losses, with a length of 5-6 ft, centered about the centerline of the beam. The reduced flange section at the location considered is uniform across the section and along the beam; the reduced section modulus is used for this portion of the beam.

- Crack at midspan in the bottom flange extending upward thru the full depth of the web plate. At that location a small element of the beam was assigned a zero moment of inertia and a negligible moment capacity.

The defects were modeled at midspan of one of the exterior girders. In addition to the dead load, two lanes of AASHTO HS20 truck loading with impact are used. The trucks are located in the same longitudinal position that would be used in normal design to compute the maximum bending moment at midspan of the girder. The dead load is applied gradually, and the truck loading is simulated by concentrated loads having the same wheel truck configuration, but only a fraction of the actual weight. This initial live loading is then incremented in the limit analysis, (a load factor of one corresponding to an HS20 loading plus impact).

Analytical Results:

50 ft span, non composite bridge : figures 8, 9, 10, and 11 show the load-deflection response of the bridge; the load deflection behavior of the defective girder G1 is shown in figure 8; the load deflection curves for the other girders , adjacent interior girder G2, interior girder G3 and exterior girder G4 are shown in figures 9, 10, and 11 respectively.

We can see that when a defect occurs in exterior girder G1, the other three girders respond to it by an increase in deflection, due to redistribution of the load; the more severe the defect, the greater the shedding of load to the other girders; we can also note that the closer the girder is to the defect the greater the distribution of load to it.

when a 50% flange loss was modeled in girder G1, a plastic hinge occurs at the midspan of the defective girder at a load factor of 2.3; at that point we observe the following response of the structure: the slab adjacent to the defect assumes an increasing amount of load until it reaches its plastic moment capacity, in the process of redistributing the load to the adjacent girder G2; a plastic hinge occurs at midspan of girder G2 at a load factor of 4.

A 100% flange loss in girder G1 caused a plastic hinge to occur in that girder at a load factor of 0.6; again the same redistribution pattern was observed: the slab adjacent to the defect picking up the load, yielding and redistributing to the other girders, mainly the closest one, interior girder G2; girder G2 develops a plastic hinge at midspan at a load factor of 3.0.

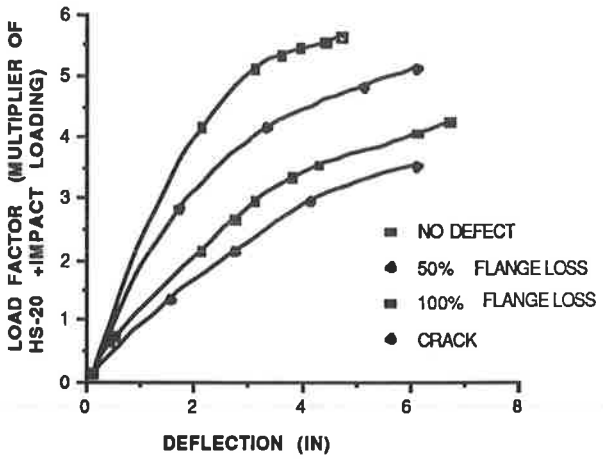

Figure 8. 50 FT Span Bridge. Load deflection curves for the defective girder G1.

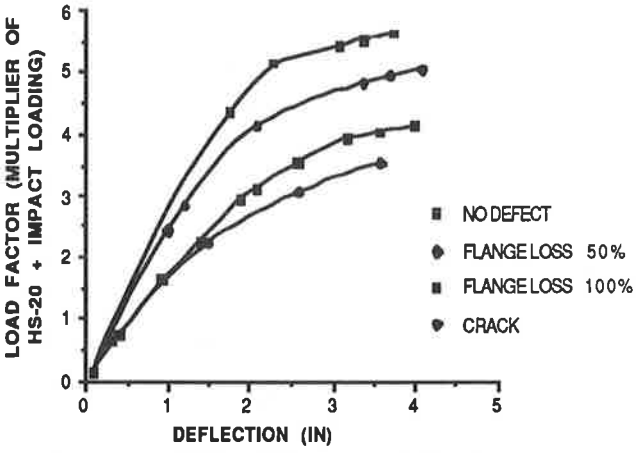

Figure 9. 50 FT Span Bridge . Load-deflection curves for interior girder G2.

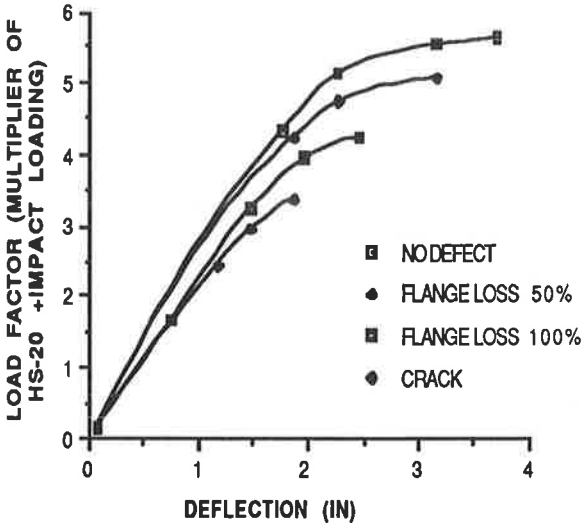

Figure 10. 50 FT Span Bridge. Load-deflection curves for interior girder G3.

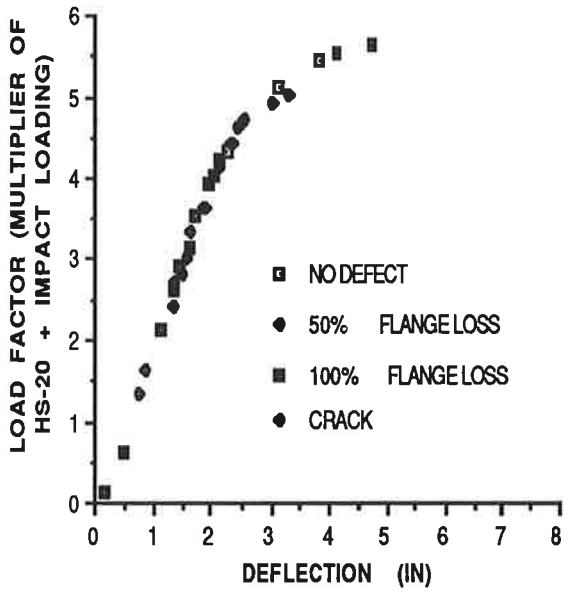

Figure 11. 50 FT Span Bridge. Load deflection curves for exterior girder G4.

A crack in girder G1 causes yielding of the adjacent slab , a first plastic hinge at midspan of adjacent girder G2 at a load factor of 2.5 , followed by a second plastic hinge in girder G2 at a load factor of 3.4 .

180 FT Span composite Bridge

The load deflection response of the bridge is shown in figures 12, 13, 14 and 15; we can see that when a defect occurs in one of the elements, in this instance girder G1, the bridge behaves as a system, and the other girders respond to the defect by assuming more load ; the more severe the defect, the more redistribution and shedding of loads to the other girders.

A 50% flange loss had little effect on the stiffness, but the reserve strength diminished; the first plastic hinge formed at midspan of the defective girder at a load factor of 2.4; this was followed by yielding and a plastic hinge forming in the diaphragm at the location of the defect; next there was formation of two plastic hinges in the adjacent girder, slab yielding at midspan near the defect location and another plastic hinge forming at midspan of girder two, at a load factor of 5.

With a 100% flange loss, the load redistribution followed the same pattern as with the 50% reduction, but with heavier yielding of the diaphragms, and further reduction in the reserve capacity.

When a crack was modeled at midspan of the exterior girder, the dead load deflection at the crack increased to 6.0 in; we observed yielding of the diaphragms and the slab in the vicinity of the crack; at a load factor of two, the adjacent girder G2 had already developed three hinges at three different locations at midspan and at the two sections where the lower flange reduces in size.

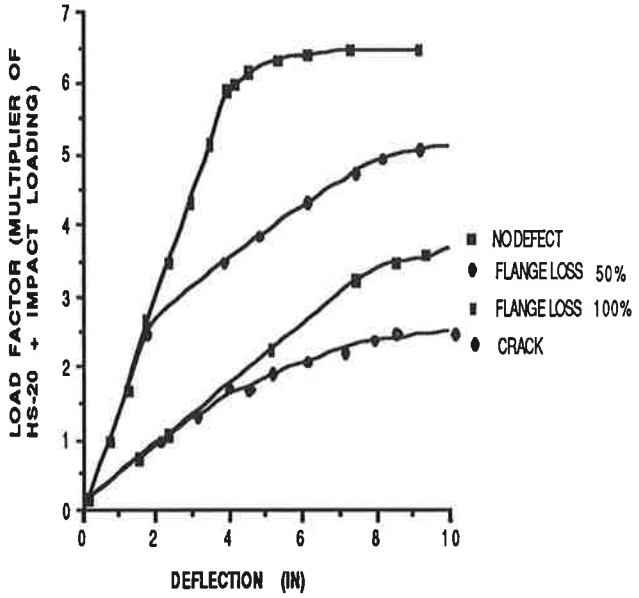

Figure 12. 180 FT Span Bridge. Load deflection curves for exterior defective girder G1.

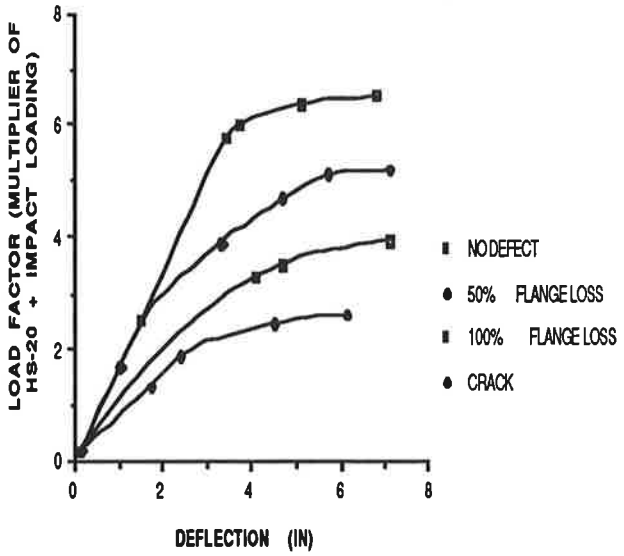

Figure 13. 180 FT Span Bridge. Load deflection curves for interior girder G2.

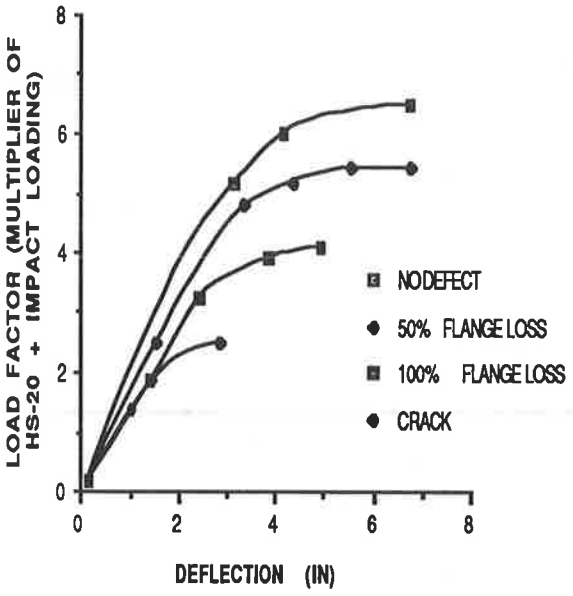

Figure 14. 180 FT Span Bridge. Load vs deflection curves for interior girder G3.

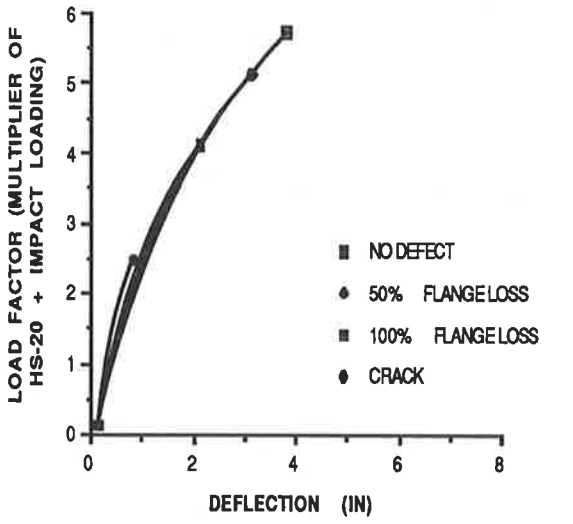

Figure 15. 180 FT Span Bridge. Load vs deflection curves for exterior girder G4.

Table 3. Maximum capacity of the 50', and 180' simple span bridges.

BRIDGE	NO DEFECT	50% FLANGE LOSS	100% FLANGE LOSS	CRACK
	LOAD FACTOR (MULTIPLIER OF HS20 + IMPACT LOADING)			
50' SPAN	5.0	4.11	3.1	3.0
180' SPAN	6.6	5.0	3.4	2.0

Summary and Conclusions

This study took a closer look at multi-girder bridge systems, their reserve capacity, and the secondary load paths present in these structures. When analyzing the overload response of the bridges studied, several conclusions could be drawn:

1. When no defect was present:
   a. The girders assumed the load, and failure occurred when all the girders had reached their ultimate capacity.
   b. The plastic flow mechanism was as follows: plastic hinges formed at first in the most stressed girders, followed by hinges occuring in the other girders.

2. When a defect was introduced:
   a. There was a change observed in the response of the bridge to load. The signs of distress in the bridge originated at the defect location in the girder, and spread first to the slab and diaphragm at the vicinity of the defect, and next to the adjacent girders; the closer the girder to the defect, the more shedding of load to it.
   b. The plastic flow pattern observed when a localized flange loss was introduced at midspan of a girder was as follows: excessive yielding and a plastic hinge forming in the girder at the defect location, followed by yielding of the slab and diaphragms at the vicinity of the defect, and then yielding and plastic hinges forming in the adjacent girders.
   c. The more extensive the defect, the more widespread and extensive the yielding was in the slab, diaphragms and girder at the vicinity of the defect. Therefore, the more severe the defect, the more load was assumed by the slab, diaphragms and adjacent girders.
   d. The multi-girder bridges considered exhibited a large reserve strength when no defect was present, several times an HS-20 truck loading. When a defect was modeled in the bridges, they still demonstrated a large reserve strength as shown in Table (3). Even when a near full depth crack was modeled at midspan of one of the main girders, the maximum capacity was 1.5 to 3.0 times an HS-20 truck loading.

References

1. Wang, C. K. "Matrix Methods of Structural Analysis", Second Edition, American Publishing, Madison, Wisconsin, 1970.

2. Yettram A.L. and Hussain H. M., " Grid-Framework Method for Plates in Flexure," Journal of the Engineering Mechanics Division, ASCE Proc.,Vol. 91, June 1965, No. EM3.
3. Traina L. A. , "Matrix Analysis of Plate Structures in Bending", Ph.D. Thesis, University of Wisconsin, Madison, 1968.
4. McCarthy W. C., "An Elastoplastic Plate Bending Finite Element with Applications to Bridge Structures", Final Report, Engineering Foundation, December 1982.
5. Melhem A. Q. "Elastic-Plastic Analysis of Composite Steel Concrete Superstructures", Ph.D. Thesis, New Mexico State University , 1986.
6. ASCE-AASHTO Task Committee " State of The Art Report on Ultimate Strength of I-beam Bridges", Journal of Structural Division, ASCE, Vol.101, May 1975,pp. 1085-1096.
7. Transportation Research Board, " Correlation of Bridge Load Capacity Estimates with Test Data", Report 306, June 1988.
8. Heins, C.P., Kato H., " Load Redistribution of Cracked Girders", Journal of Structural Engineering, ASCE, Vol.108, August 1982, pp.1909-1915.
9. Halls, J.C., Kostem,C.N. "Inelastic Analysis of Steel Multi-Girder Highway Bridges", Fritz Engineering Lab Report No.435.1, Lehigh University, Bethlehem, Pennsylvania,1980.
10. Schwendeman L. P. , Hedgren A. W. Jr. , "Bolted Repair of Fractured I-79 Girder",Journal of the Structural Division, ASCE, Vol. 104, No. ST10, Proc. Paper 14083. Oct., 1978, pp. 1657-1670.
11. Standard Specifications for Highway Bridges, AASHTO Code, 13th ed.,American Association of State Highway and Transportation Officials,1983.
12. Daniels, J.H., Kim, W., and Wilson, J.L., "Recommended Guidelines for Redundancy Design and Rating of Two-Girder Steel Bridges", NCHRP Report 319 (1989).
13. Heins,C.P., Hou,C.K., "Bridge Redundancy: Effects of Bracing", Journal of the Structural Division, Vol. 106,No. ST6, June, 1980, pp. 1364-1367.
14. Burdett,E.G., AND Goodpasture, D.W., "Full Scale Bridge Testing: An Evaluation of Bridge Design Criteria", University of Tennessee, December 1971.
15. Highway Research Board, "The AASHTO Road Test: Report 4, Bridge Research", Highway Research Board Special Report 61D, 1962.